Electronic Supplementary Material (ESI) for Journal of Materials Chemistry C

Supporting Information

Efficient All Polymer Solar Cells from Layer-evolved Processing of a Bilayer Inverted Structure

Kai Yao, Jeremy J. Intemann, Hin-Lap Yip, Po-Wei Liang, Chih-Yu Chang, Yue Zang, Yiwang Chen* and Alex K.-Y. Jen*

Experimental Section

OPV Device Fabrication and Characterization: ITO-coated (15 Ω/sq) glass substrates were cleaned sequentially with a detergent, DI-water, acetone, and isopropanol. Prior to the fabrication of the organic layers, the ITO surface was treated with UV-Ozone. For the conventional structure OPVs, PEDOT:PSS (Baytron 4083) was first deposited on these ITO substrates (~ 40 nm) and then baked at 140 ^oC for 10 min. The BHJ active layers (ca. ~100 nm) were spin-cast in a N_2 filled glove box from a solution of P3HT:PIDSe-DFBT (with different weight ratios) in dichlorobenzene, with the overall concentration of 15 mg/ml. After spin-coating the photoactive layers, all the samples were thermally annealed at 140 ^oC for 10 min. Then the film was transferred into a thermal evaporator that is located in the same glove box. A Ca layer (20 nm) and an Al layer (100 nm) were deposited in sequence under high vacuum ($<2 \times 10^{-6}$ Torr) to serve as cathode. As for the devices with an inverted structure, the prepared ZnO sol-gel was spin-coated on the pre-cleaned ITO-coated glass substrate at 4000 rpm. The ZnO films were annealed at 200 °C for 1 h in the air. The C60-SAM was deposited on the ZnO surface using a two-step spin process, while the PFN-Br and PEIE solution was spin cast on the ZnO at a spin rate of 4000rpm and 5000rpm for 1 min, respectively. Afterward, the sequentially processed bilayer active layer in the inverted structure devices was prepared. For the optimized device, the PIDSe-DFBT solution with a concentration of 7.5 mg/ml in DCB co-solvent was spin-coated on top of the PEDOT:PSS layer at 1000 rpm for 40 s and then a P3HT solution of 4 mg/ml with 0% to 20% CB co-solvent in DCM was also directly spin-coated on top of the PIDSe-DFBT layer at 1500 rpm for 40 s. The bilayer or LE-Bilayer devices were dried at 140^{o}C for 10 min in a glove box. After annealing, 10 nm MoO_3 and 100 nm Ag were deposited sequentially under high vacuum by thermal evaporation. All the *J*-*V* curves in this study were recorded using a Keithley 2400 source measure unit. The device photocurrent was measured under illumination from a 450 W Thermal Oriel solar simulator

(AM1.5G). The illumination intensity of the light source was accurately calibrated employing a standard Si photodiode detector equipped with a KG-5 filter, which can be traced back to the standard cell of the National Renewable Energy Laboratory (NREL).The EQE spectra performed here are obtained from the IPCE measurement using the combination of a Xenon lamp (Oriel, 450 W) as the light source, a monochromator, chopper with frequency of 100Hz, a lock-in amplifier (SR830, Stanford Research Corp), and a Si-based diode (J115711-1-Si detector) for calibration. The absorption and transmission spectra were measured using a Perkin-Elmer Lambda-9 UV-visible spectrophotometer. Tapping-mode AFM images were taken on a Veeco multimode AFM with a Nanoscope III controller.

Device Fabrication and Characterization of FET: Field-effect transistors were fabricated through the top-contact and bottom-gate geometry. Heavily doped p-type silicon <100>substrates with a 300 nm thermal oxide layer were purchased from Montco Silicon Technologies INC. After cleaning the substrate by sequential ultra sonication in acetone and isopropyl alcohol for 15 min followed by air plasma treatment, the oxide layer was passivated with a thin divinyltetramethyldisiloxane-bis(benzocyclobutene) (BCB) buffer layer. Polymer thin films were spin-coated from a 0.5 wt % DCB solution. Interdigitated source and drain electrodes (W=1000 μm, L= 20/30 μm) were defined by evaporating a Au (40 nm) through a shadow mask from the resistively heated Mo boat at 10^{-7}Torr. OFET characterization was carried out in a N_2–filled glove box using an Agilent 4155B semiconductor parameter S6 analyzer. The field-effect mobility was calculated in the saturation regime from the linear fit of $(I_{ds})1/2$ vs V_{gs}. The threshold voltage (V_t) was estimated as the x intercept of the linear section of the plot of $(I_{ds})1/2$ vs V_{gs}. The sub threshold swing was calculated by taking the inverse of the slope of I_{ds} vs V_{gs} in the region of exponential current increase.

SCLC Mobility measurements: Space charge limited currents have been tested in electron only devices with a configuration of ITO/Al/PIDSe-DFBT:P3HT/Ca/Al and hole-only devices with a configuration of ITO/PEDOT:PSS/PIDSe-DFBT:P3HT/MoO_3/Au. The devices were prepared following the same procedure described in the experimental section for photovoltaic devices, except that of the metal electrode. The mobilities were determined by fitting the dark current to the model of a single carrier SCLC current with field dependent mobility, which is described as

$$J = \frac{9\varepsilon_r\varepsilon_0\mu_0 V^2}{8L^3}\exp(\beta\sqrt{\frac{V}{L}})$$

where J is the current, μ_0 is the zero-field mobility, ε_0 is the permittivity of free space, ε_r is the relative permittivity of the material, V is the effective voltage, and L is the thickness of the active layer.

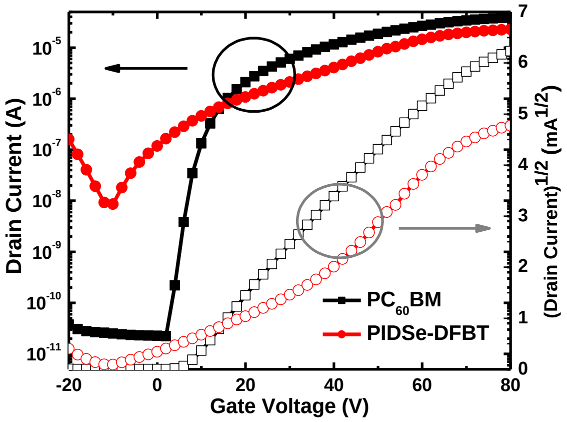

Figure S1. Transfer curve of spin-coated PIDSe-DFBT and PC$_{60}$BM thin film transistors.

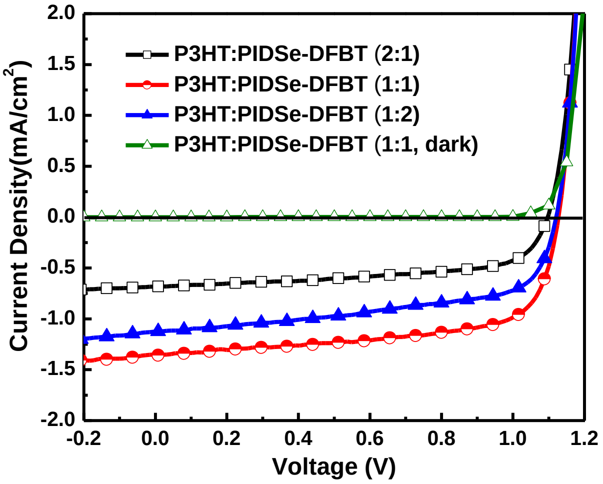

Figure S2. J−V curves of conventional BHJ device using various blending ratios of PIDSe-DFBT:P3HT under AM 1.5100 mW/cm^2 illumination and the dark condition of 1:1 ratio device.

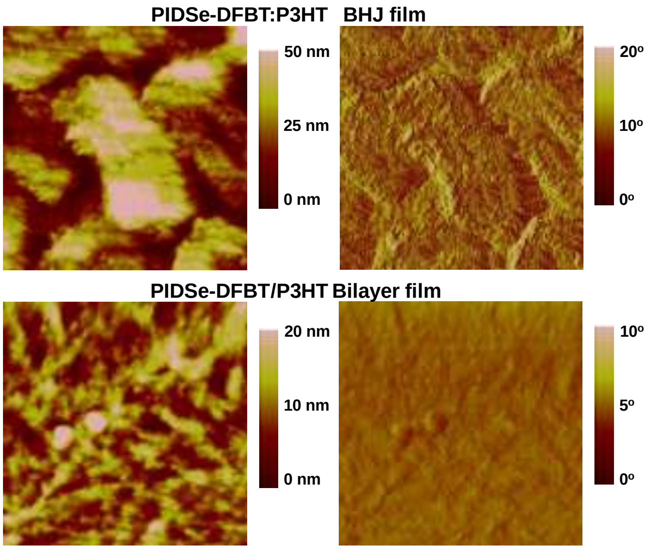

Figure S3. Top-down AFM height (left) and phase (right) images (2 μm by 2 μm) of PIDSe-DFBT:P3HT blend film and PIDSe-DFBT/P3HT bilayer film.

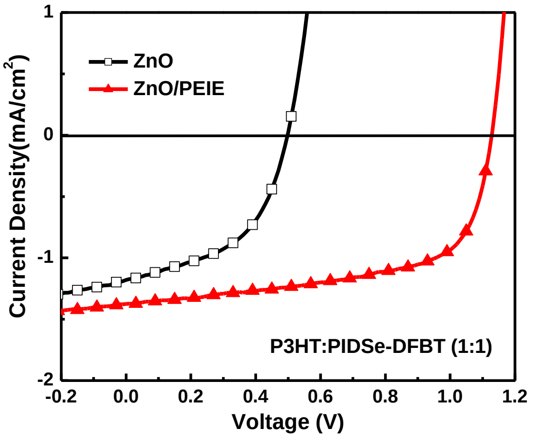

Figure S4. $J-V$ curves of inverted BHJ device using different electron-transporting layers at the blending ratio of PIDSe-DFBT:P3HT (1:1) under AM1.5 (100 mW/cm^2) illumination.

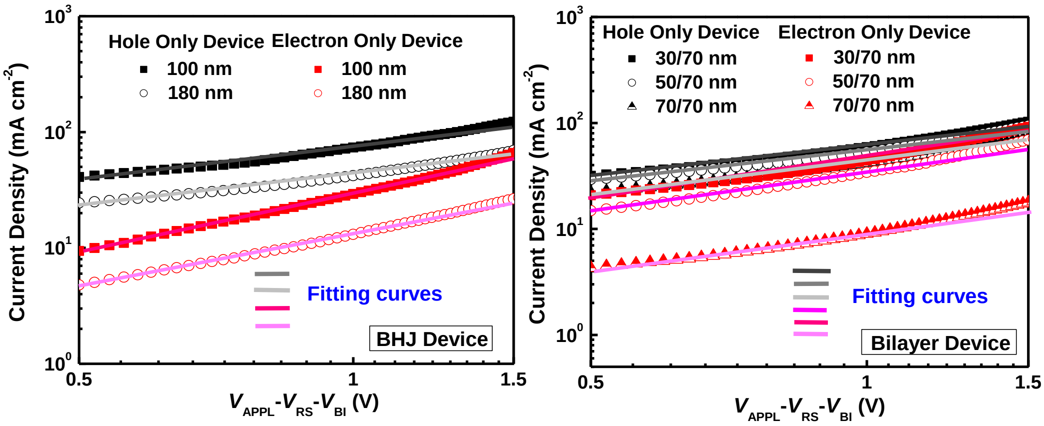

Figure S5. The J–V characteristics of electron and hole only devices in different structures and activelayer thickness. The biasis corrected for built-in Voltage V_{Bi}, arising from difference in the work function of thecontacts, and the voltage drop due to substrate series resistance, such that $V = V_{APPL} - V_{RS} - V_{Bi}$. The solid lines represent the fitting curves.

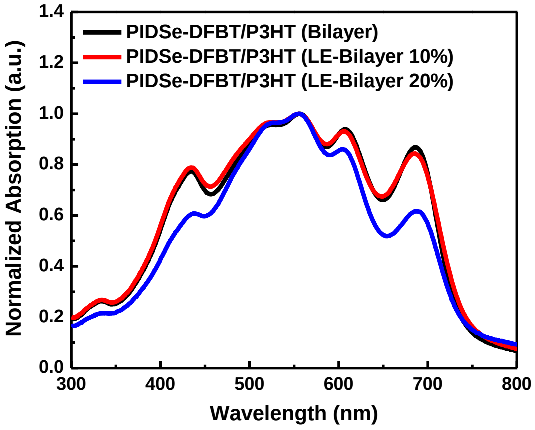

Figure S6. Absorption spectra of PIDSe-DFBT/P3HT films prepared by bilayer mixture (100 wt % CH_2Cl_2 without co-solvent) and co-solvent (10% and 20% CB) layer-evolved bilayer (LE-bilayer).

Table S1. Comparison of performance parameters of the conventional and inverted BHJ devices under AM1.5 illumination.

Device	*J*sc[mA cm^{-2}]	*V*oc[V]	FF [%]	η[%]
PIDSe-DFBT:P3HT (2:1)[a]	1.13	1.12	58.2	0.73
PIDSe-DFBT:P3HT (1:1)[a]	1.34	1.13	65.7	0.99
PIDSe-DFBT:P3HT (1:2)[a]	0.68	1.10	60.7	0.45
PIDSe-DFBT:P3HT (1:1)[b]	1.38	1.13	61.6	0.96
PIDSe-DFBT:P3HT (1:1)[c]	1.18	0.49	50.9	0.30

[a] Conventional structure. [b]Inverted configuration using PEIE/ZnO; [c] Inverted configuration using ZnO.

Table S2. Performance parameters of bilayer device[a] at various thickness of PIDSe-DFBT layers (based on the solution concentrations) under AM1.5 illumination.

PIDSe-DFBT	P3HT	*J*sc [mA cm^{-2}]	*V*oc [V]	*FF* [%]	η [%]
4.5 mg/ml (30 nm)	4 mg[b] (70 nm)	2.72	0.47	48.2	0.62
7.5 mg/ml (50 nm)	4 mg/ml	3.18	0.48	49.4	0.75
10 mg/ml (70 nm)	4 mg/ml	2.49	0.49	47.5	0.58

[a]Inverted device configuration using ZnO electron-transporting layer. [b]The 4 mg/ml is the largest solubility of P3HT in warm DCM.

Table S3. Summary of the derived fitting data for the single charge transport devices based on Mott-Gurney law

Device	Hole mobility [cm^2 V^{-1} s^{-1}]	Electron mobility [cm^2 V^{-1} s^{-1}]
BHJ Device (1:1)	1.1×10^{-3}	5.6×10^{-5}
	Bilayer Device	
P3HT/PIDSe-DFBT (70/30nm)	9.6×10^{-4}	8.6×10^{-4}
P3HT/PIDSe-DFBT (70/50nm)	9.5×10^{-4}	8.3×10^{-4}
P3HT/PIDSe-DFBT (70/70nm)	9.9×10^{-4}	1.1×10^{-4}